

# Application of Visual Communication Technology in Image Enhancement and Optimization of Human Machine Interaction Interface

Xiping Wu

\*Corresponding author's e-mail: wuxiping@163.com

Wuxi Vocational institute of Commerce, Wuxi 214153, China

**Abstract.** To address the technical issues in the design process of traditional human-computer interaction systems, a human-computer interaction system design based on visual communication technology is implemented. Firstly, for the skin color detection method in color space, a neural network color filter based on fuzzy patterns is created based on the BP neural network model based on the threshold changes of different lighting conditions. The filter designed in this paper has a fast learning speed and can be used in vast lighting conditions and complex environments. Moreover, the human-computer interaction system has been meticulously crafted to align seamlessly with users' accustomed practices. Leveraging the EC5-1719CLDNA embedded star as its hardware foundation, the system integrates a compact projection unit and a radiation control system. On the software front, a paperless office interaction engine has been developed, making optimal use of the robust computational capabilities offered by multithreading and the selected hardware platform. Subsequently, rigorous testing was conducted, affirming that the system not only meets but surpasses the specified operational demands.

**Keywords:** Visual communication technology; Human machine interaction; Interface image; application

## 1. Introduction

Human Computer Interaction (HCI) technology mainly focuses on the research of computers, humans, and mutual influence technologies, and has fully demonstrated the potential of this field, such as geospatial tracking technology designed in smartphones; Action recognition technology used in wearable computers, immersive devices, stealth technology, etc; Applying silent speech recognition to individuals with language barriers. Although it has good potential for use, it still faces certain challenges, such as poor real-time performance and low recognition rate of visual gestures[1]. So, it is necessary to conduct research on multiple algorithms to improve recognition accuracy and speed, but the scope of their use has not been widely limited. With the rapid development of information technology, human-computer interaction interfaces play an increasingly important role as a bridge between users and computer systems. In this digital age, interface design is not only related to the quality of user experience, but also directly affects the acceptance of products or services by users. In the process of human-computer interaction, images, as an important means of information transmission, play the role of intuitive, vivid, and efficient communication tools[2]. Visual communication technology, as an important component of image design and processing, plays

a crucial role in enhancing and optimizing human-computer interaction interface images. By utilizing advanced image processing algorithms, graphic design principles, and scientific principles of visual perception, visual communication technology can effectively improve users' perception and understanding of interface information, and enhance their interactive experience. This paper will explore the utilization of visual communication technology to enhance images within human-computer interaction interfaces, aiming to optimize the overall user experience[3].

## 2. Overall plan of the system

The core of the system is built upon the robust EC5-1719CLDNA Embedded Star, supported by advanced radiation control systems and compact mini projection systems. Redefining user input, it employs an innovative laser-enhanced reflection non-deterministic surface multi-touch technology, ushering in a new era by replacing traditional mouse and touch screen components. This groundbreaking approach ensures a fluid human-computer interaction experience, seamlessly adapting to both home entertainment and office environments without the need for standard accessories. The software backbone is crafted in Java, ensuring adaptability across diverse platforms. The distinct software architecture is designed for functional scalability, guaranteeing a versatile user experience. Functionalities include efficient image browsing, multi-user participation, office recording, and diverse multi-interface modes, offering a comprehensive solution for both professional and leisure scenarios[4]. Notably, the system's design sets the stage for future enhancements, with upcoming iterations poised to introduce features such as seamless file transfer and collaborative user capabilities. Figure 1 provides a visual representation, offering a holistic view of the system's intricate framework.

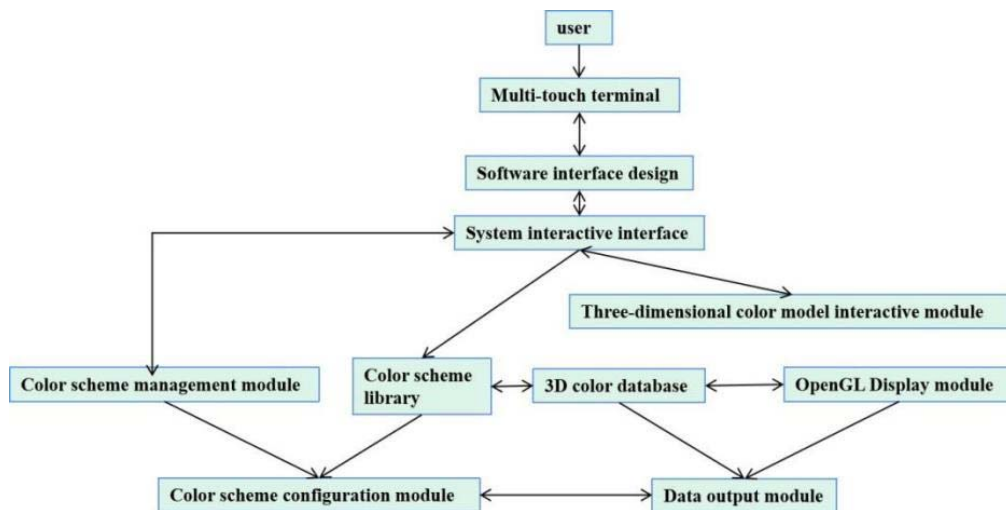


Figure 1. Overall framework of the system

### 3. Design of human-machine interaction system

#### 3.1. Visual perception and color configuration

##### (1) Visual perception of signs

Visual perception of signs refers to both human physiological perception and emotional experience of signs. Physiological perception is the most objective response of people to signs, while emotional experience is the thoughts that people react to signs; The physiological perception of signs is simply the perception of color, and this process is relatively short. Visual perception also has a corresponding perception of color. From the perspective of logo design, this perception includes a sense of volume, temperature, and distance. Standard emotional experience refers to the visual perception that is deeper than physiological perception, mainly manifested in the physiological perception of logo color and the emotional judgment of the brain through analysis combined with its own experience on the logo.

##### (2) The Role of Visual Perception in the Configuration of Logo Colors

To establish a color configuration, the initial step involves comprehending the visual perception associated with the primary and accent colors, along with the harmonious and contrasting elements within the logo. The main color (M) is categorized into two types: vivid color (M1) and deep color (M2). The three auxiliary color (A) configurations consist of primary color (Am), contrasting color (A2), and harmonious color (A1). Employing a 2×3 combination approach yielded six potential color schemes; however, due to variations in harmonic colors and primary colors, only four viable color configurations emerged. The amalgamation of two distinct visual perceptions results in diverse visual effects through different color configurations [5].

The logo's main color and auxiliary color establish a hierarchical relationship, with the former holding dominance over the latter. Recognizing this dominance, the study assigns weight values to each, acknowledging the greater significance of the main color. All main colors are monochromatic, devoid of spatial or gravitational cues in physiological perception, only evoking a sense of temperature. The contrast between these two colors is pronounced, featuring distinct and vibrant hues. Visual perceptions of color configuration schemes are detailed in Table 1.

**Table 1.** Color Configuration Scheme

Color configuration scheme	Physiological perception	Emotional experience	
Programme 1	M1A1	Cold, heavy and far	Excitement, lightness, technology
	M1A1	Cold, heavy and far	Quiet, solemn and classical
	M1A2	Cold, light and close	Excitement, lightness, technology
Programme 2	M2A 1	Warm, heavy and far	Warm, heavy and far
	M2A2	Warm, light and close	Quiet, solemn and classical
	M2A2	Warm, light and close	Excitement, lightness, technology

#### 3.2. Enhance local contrast of images

Local contrast enhancement methods need to be used to enhance the contrast of high-frequency areas in laser imaging images. Select 3 \* 3 pixels from the original laser X-ray

imaging image to enhance local contrast[6]. The method used in this process is local statistical method, and the expression is shown in equation (1):

$$f(i, j) = \bar{h}(i, j) + k * [h(i, j) - \bar{h}(i, j)] \quad (1)$$

In the formula,  $h(i, j)$  and  $f(i, j)$  represent the brightness values of the input and output, respectively. The neighborhood average value is described as  $\bar{h}(i, j)$ , and  $k$  is the gain coefficient.

By using equation (1) to enhance the contrast of laser imaging images, the local mean of a certain point in the image will not be changed. However, increasing the contrast will increase the standard deviation of the laser imaging image by  $k$  times. The contrast enhancement effect of laser imaging images is directly proportional to the  $k$  value. If the  $k$  value is small, it will cause the laser imaging image to be blurry. If the  $k$  value is large, it will improve the clarity of the laser imaging image. Therefore, researchers usually set the  $k$  value to 0.75 value 1 Between 05[7].

### 3.3. Color image enhancement algorithm based on visual characteristics

#### 1) Overall brightness adjustment

To globally fine-tune the brightness of the two-dimensional visual image in the human-computer interaction interface, a key methodology revolves around nonlinear adaptive histogram stretching. The focal point of this technique is the augmentation of darker regions within the interface. This is executed by assigning the brightness component  $MaxRGB(i, j)$  of the planar visual image to the maximum value among the trio of primary colors—R, G, and B. The operational essence of this process can be encapsulated through the expression illustrated in equation (2):

$$MaxRGB(i, j) = \max(OriR(i, j), OriG(i, j), OriB(i, j)) \quad (2)$$

Within the equation, the RGB components (R, G, and B) associated with the pixel located at coordinates  $(i, j)$  in the RGB space of the original image are symbolized as  $OriR(i, j)$ ,  $OriG(i, j)$ , and  $OriB(i, j)$ , respectively. The procedural aspect entails arranging the grayscale values in  $MaxRGB(i, j)$  for pixels surpassing the specified threshold, denoted as  $\omega$ , indicated by the count  $m$ . The threshold  $\omega$  is precisely defined in equation (3):

$$\omega = \text{uint8}(Long * Width * \frac{100}{266}) \quad (3)$$

In the given equation, the term `uint8` signifies an 8-bit unsigned positive number represented in binary. The image dimensions are parameterized by `Length` and `Width`, with 266 indicating the count of gray values, and 100 serving as the threshold value. Notably, pixels with gray values below the threshold are exempt from the sorting process, mitigating the influence of a limited number of gray values on the overall mapping. The mapping of gray values adheres to an exponential mapping function, succinctly articulated in expression (4):

$$TraRGB(i, j) = 266 * (m - 1) / (m - 2) * g1 \quad (4)$$

## 2) Local contrast enhancement

After the thorough brightness adjustment, the intricate details within the broader low-illumination regions of the image can be highlighted. Subsequently, the local contrast of image brightness is improved by leveraging the correlation among gray values of pixels within a specific region, resulting in a more pronounced depiction of image details denoted as  $R'$ .

The average brightness within a  $9 \times 9$  window size is computed, and the utilization of a median filter ensures the preservation of edge details in the image. Hence, the mean brightness within this range is calculated using the median filtering method, as expressed in equation (5):

$$MedRGB(i, j) = median(TraRGB(i, j)) \quad (5)$$

Once the brightness average is computed through the aforementioned formula, the enhancement of local color contrast in the image is achieved through the application of formula (6):

$$ResRGB(i, j) = g_2(TraRGB(i, j) - MedRGB(i, j) + TraRGB(x, y)) \quad (6)$$

In this context, setting  $g_2$  to 2,  $TraRGB(i, j)$  characterizes the pixel's gray value after the comprehensive brightness processing. Furthermore,  $MedRGB(i, j)$  denotes the average brightness within the designated region. The outcome,  $ResRGB(i, j)$ , represents the gray value following the local contrast enhancement. This correlation is visually depicted in the explanatory Figure 2:

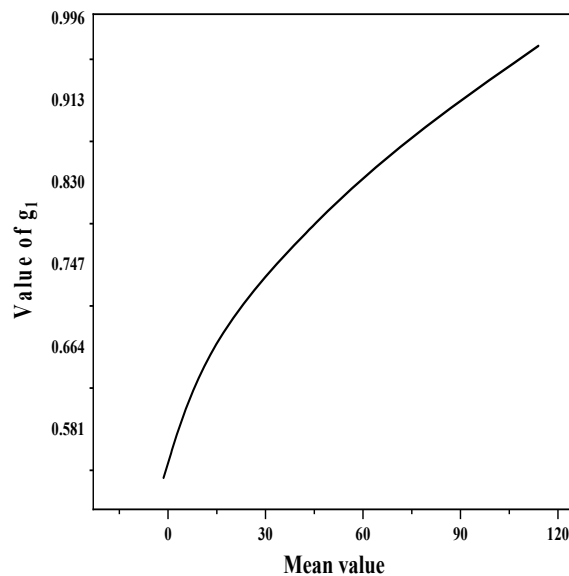


**Figure 2.** The functional relationship between  $G_1$  and the mean

## 4. Testing and Verification Plan

Using the electrician laboratory as the testing environment, a computer and anti-static experimental table are configured in the laboratory, which also includes one signal generator, spectrum analyzer, handheld multimeter, 50MHz oscilloscope, and two voltage stabilizing sources. The key function implementation includes: testing the arm posture sensor, wearing gloves to the right hand, requiring the forearm to be parallel to the ground, with the palm facing downwards, and rotating the forearm 120° based on the elbow. This action is repeated, and the sensor data waveform can be obtained through a virtual oscilloscope [8]. From the test results, it can be seen that the finger bending sensor exhibits significant fluctuations. By enabling gestures to match different semantics in a short period of time, the relay device can control the electrodes and steering gear, and the wearer can directly control the device. The steps to adjust the control gesture are as follows: shift the hand in the controlled device, then enter the device selection mode, and hold the fist with one hand to make the device control state contact the device to maintain the previous control quantity; If an unexpected situation occurs during use, press the emergency brake on the relay board TSI, or make all equipment emergency stop. Afterwards, reliability testing was conducted on the system designed in this article, wearing gloves in a fully charged state and repeating internal demand actions. Sending posture encoding in the upper computer and comparing gesture sequences resulted in 431 sets of data, of which 73 sets of data bits did not match, with an accuracy rate of 82%. The system works stably during this process, and there are no issues with sending programs or hardware errors. It has strong electromagnetic interference and strong adaptability to static electricity and other environments [9-10].

## 5. Conclusion

At the heart of the system lies the EC5-1719CLDNA Embedded Star, serving as the cornerstone of its hardware architecture. The integration encompasses radiation control systems and compact mini projection systems. A pioneering approach is adopted with laser-enhanced reflection non-deterministic surface multi-touch technology, redefining user input and displacing conventional mouse and touch screen components. This transformative technology facilitates fluid human-computer interaction, catering to both home entertainment and office functionalities in various settings, thereby obviating the need for typical accessories. The software interaction systems are implemented using the Java language, ensuring portability across different platforms. A distinctive software architecture design is in place to guarantee functional scalability. The system designed in this article utilizes a new design concept to interpret the concept of human-computer interaction, overturning the traditional single person, vertical human-computer interaction and based on the standard input device interaction mode, improving the user experience through a more suitable way for people's habits. The system fully demonstrates good application prospects in software functionality scalability, recognition accuracy, real-time interaction, and other aspects.

**Acknowledgments:** 2022 General Project of Philosophy and Social Science Research in Jiangsu Province Universities "Research on the Transformation Path of Traditional Art Resources in Jiangsu Grand Canal Cultural Belt", Project Number: 2022SJYB1055

## References

- [1] Yun, B. . (2021). Design and reconstruction of visual art based on virtual reality. *Security and Communication Networks*, 2021(8), 1-9.
- [2] Pan, L. , Sun, G. , Chang, B. , Xia, W. , Jiang, Q. , & Tang, J. , et al. (2023). Visual interactive image clustering: a target-independent approach for configuration optimization in machine vision measurement. *Frontiers of Information Technology & Electronic Engineering*, 24(3), 355-372.
- [3] Katamine, E. , Kawai, R. , & Yamashita, H. . (2021). Shape optimization of viscous flow field considering fluid-structure-interactive. *Transactions of the JSME (in Japanese)*, 87(899), 21-00116-21-00116.
- [4] JieLIU, Pin-hongYOU, MingTIAN, & Jin-fengLIU. (2022). Smooth optimization of parallax images mosaic based on local projection. *Acta Electronica Sinica*, 50(06), 1451-1456.
- [5] Liang, R. , Fan, J. , & Yue, J. . (2021). A cascaded multi-irss beamforming scheme in mmwave communication systems. *IEEE Access*, PP(99), 1-1.
- [6] Kim, T. , Kwon, T. , Lee, J. , & Song, J. . (2021). F/wvis: hierarchical visual approach for effective optimization of firewall policy. *IEEE Access*, PP(99), 1-1.
- [7] Li, C. , Wang, Z. , Tong, H. , Tian, S. , & Yang, L. . (2022). Optimization of the number and positions of fixture locators for curved thin-walled parts by whale optimization algorithm. *Journal of Physics: Conference Series*, 2174(1), 012013-.
- [8] Brand, F. , Dendler, L. , Fiack, S. , Schulze, A. , & Bl, G. F. . (2022). Risk communication of policy advising scientific organisations: athematic outline using the example of the german federal institute for risk assessment. *Bundesgesundheitsblatt, Gesundheitsforschung, Gesundheitsschutz*, 65(5), 599-607.
- [9] Chiang, J. C. , Shih, W. H. , & Deng, J. Y. . (2021). Rate-distortion optimization of multi-exposure image coding for high dynamic range image coding. *Signal Processing Image Communication*, 95(3), 116238.
- [10] Iida, H. , & Imai, J. I. . (2023). Improvement of flick input interface using hand tracking in vr environments. *Transactions of the Society of Instrument and Control Engineers*, 59(2), 51-61.